JACS
JOURNAL OF THE AMERICAN CHEMICAL SOCIETY

COMMUNICATION

pubs.acs.org/JACS

Early Stages of Crystallization of Calcium Carbonate Revealed in Picoliter Droplets

Christopher J. Stephens,[†] Yi-Yeoun Kim,[‡] Stephen D. Evans,[†] Fiona C. Meldrum,[*,‡] and Hugo K. Christenson[*,†]

[†]School of Physics and Astronomy and [‡]School of Chemistry, University of Leeds, Leeds LS2 9JT, United Kingdom

Supporting Information

ABSTRACT: In this work, we studied the heterogeneous nucleation and growth of $CaCO_3$ within regular arrays of picoliter droplets created on patterned self-assembled monolayers (SAMs). The SAMs provide well-defined substrates that offer control over $CaCO_3$ nucleation, and we used these impurity-free droplet arrays to study crystal growth in spatially and chemically controlled, finite-reservoir environments. The results demonstrate a number of remarkable features of precipitation within these confined volumes. $CaCO_3$ crystallization proceeds significantly more slowly in the droplets than in the bulk, allowing the mechanism of crystallization, which progresses via amorphous calcium carbonate, to be easily observed. In addition, the precipitation reaction terminates at an earlier stage than in the bulk solution, revealing intermediate growth forms. Confinement can therefore be used as a straightforward method for studying the mechanisms of crystallization on a substrate without the requirement for specialized analytical techniques. The results are also of significance to biomineralization processes, where crystallization typically occurs in confinement and in association with organic matrices, and it is envisaged that the method is applicable to many crystallizing systems.

Crystallization is an important topic that is central to fields as diverse as pharmaceuticals and nanomaterials, scale formation, corrosion and weathering, and analysis of protein structures. In all cases, progress depends on determining the mechanisms by which crystal nucleation and growth occur. Biominerals, with their hierarchical structures and highly controlled features such as lateral spatial distribution, polymorphism, and morphology,[1,2] provide beautiful examples of the degree of control that can be exerted over crystallization processes. It is well-recognized that organic molecules, as either soluble additives[3−5] or insoluble organic matrices,[6−10] are employed to control biomineral formation in nature. A further feature of these systems that is often neglected but has tremendous potential for use in crystallization control is the fact that biomineralization inevitably occurs within well-defined microenvironments.[11,12] While some of the consequences of such compartmentalization are clear, such as the provision for selective uptake of ions or precursor species into the mineralization environment, the influence of confinement on biomineralization processes is currently poorly understood.

In this work, we investigated the effect of confinement on calcium carbonate precipitation by carrying out crystallization within arrays of picoliter droplets supported on functionalized patterned self-assembled monolayers (SAMs). This system provides a unique opportunity to study heterogeneous nucleation and crystal growth in environments where both the volume and reservoir are restricted, and it is therefore quite distinct from templating systems such as membrane pores,[12] porous polymers,[13,14] or wedges,[11] which offer confinement but are still open to the bulk solution. The results demonstrate that these restricted reaction volumes have a number of significant effects on the precipitation reaction. First, crystallization of $CaCO_3$ is retarded in these small-volume droplets in comparison with bulk solution, and second, the growth process terminates early because of the finite reservoir conditions, thereby revealing intermediate growth forms of calcite. Such droplet arrays therefore provide a unique and accessible method for investigating the early stages of precipitation.

Carrying out crystallization in impurity-free small droplets is well-recognized as a method for studying homogeneous nucleation[15,16] and has most frequently been used for protein crystallization, with the reported advantages of an increase in crystal stability and ease of theoretical predictions.[17,18] Droplet microfluidic systems are also being developed for precipitation of proteins[19] and a number of other substances under conditions of homogeneous nucleation.[20] Of relevance to the current work, $CaCO_3$ precipitation was studied in millimeter-scale levitated droplets, where solution-created amorphous calcium carbonate (ACC) was shown to adsorb to and then be transformed into calcite at the interface.[21] In specific regard to heterogeneous nucleation, droplet arrays on patterned SAMs were recently employed by Myerson and co-workers[22,23] to investigate the polymorphism of the organic compounds glycine, sulfathiazole, and mefenamic acid. The last of these systems was quite distinct in both method and goal from our experiments in that significantly larger nanoliter droplets were employed and crystallization was induced upon evaporation of the droplets. The very high evaporation rates achieved provided access to different polymorphs.

SAMs offer many advantages for supporting the formation of droplet arrays because of their ordered structure, modifiable functionality, and relative stability under ambient conditions and the fact that they can be readily patterned using conventional lithography techniques, yielding chemically patterned microarrays with a submicrometer edge resolution. They have also been extensively studied as model organic assemblies for templated crystallization of $CaCO_3$, where they have been shown to

Received: January 12, 2011
Published: March 22, 2011

dx.doi.org/10.1021/ja200309m | J. Am. Chem. Soc. 2011, 133, 5210–5213

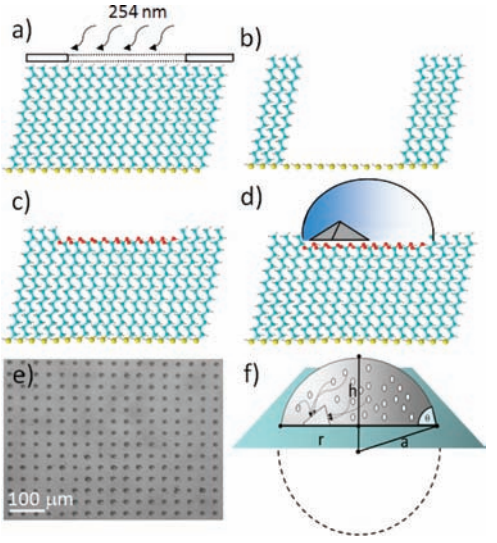

Figure 1. Schematic diagram of the fabrication of the droplet arrays. (a) A 1*H*,1*H*,2*H*,2*H*-perfluorodecanethiol self-assembled monolayer deposited on a gold-on-mica substrate is exposed to λ = 254 nm UV light through a quartz photomask with arrays of circular holes. (b) Removal of irradiated alkyl thiols with solvent. (c) "Backfilling" of exposed regions with mercaptohexadecanoic acid (MHA) solution, yielding a patterned surface comprising hydrophilic circles on a hydrophobic background. (d) Deposition of droplets by passing a $Na_2CO_3/CaCl_2$ solution across the patterned SAM at 100% humidity. (e) Optical image of an array of 10 μm radius droplets. (f) Individual droplet with radius *a*, height *h*, base radius *r*, and contact angle θ on the substrate.

support highly efficient face-selective nucleation of calcite.[7,8] Here, SAMs of fluoroalkylthiols on Au were patterned using "deep" UV photolithography and backfilled with carboxylic acid-terminated alkylthiols, yielding circular hydrophilic regions with radii of 4−10 μm on a hydrophobic background (Figure 1). Supersaturated aqueous solutions of $CaCO_3$ were then passed across the microengineered surfaces, trapping solution on the hydrophilic areas and leading to arrays of up to 20 000 independent droplets, which were stable for days at 100% humidity.

Examination of crystallization in these arrays after 24 h revealed that the vast majority of droplets contained a single crystal of $CaCO_3$ (Figure 2a). For example, in the case of the 10 μm radius droplets, while >90% of the droplets contained a single crystal, an average of seven rhombohedral calcite crystals, mainly in (012) or (015) orientations, formed in each hydrophilic domain when a patterned substrate was immersed in bulk solution, where the quantity of reagents was unrestricted (Figure 2b). Comparison of samples with different-sized droplets showed that the occupancy and projected particle area (i.e., the area of the crystal face in contact with the substrate) were dependent on the surface area of the base of the droplet, whereas multiple occupancy of the droplets was independent of droplet size (Table 1) for the range of droplet diameters investigated. Although the crystallites frequently appeared to be located near the edges of the circular patterns (Figure 2a), the fact that the crystallites were oriented (see below) rules out nucleation at the droplet−water interface or displacement of the crystals during removal of the droplets.

The crystals that precipitated within the droplets were identified as calcite on the basis of their morphologies and were

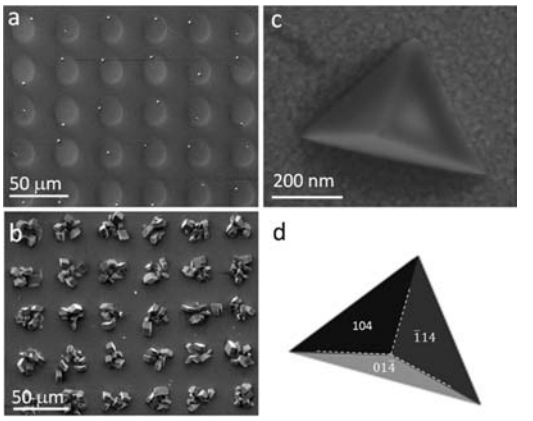

Figure 2. (a, b) SEM images showing $CaCO_3$ precipitated from (a) single droplets and (b) bulk solution onto surfaces patterned with 10 μm radius circles. (c) Enlarged image of a representative calcite tetrahedron precipitated within a single 5 μm radius droplet after 24 h, oriented with a {012} nucleation face. (d) Simulated calcite tetrahedron oriented with a {012} nucleation face, as defined by a single threefold axis with projected angles of 142, 104, and 104°.

Table 1. Key Data for $CaCO_3$ Precipitation in Droplets

	droplet radius		
parameter	10 μm	5 μm	4 μm
droplet base area (μm^2)	314	78.5	50
droplet volume (pL)[a]	0.688−2.094	0.086−0.262	0.044−0.134
total $CaCO_3$/droplet (fL)	0.13−0.39	0.016−0.048	0.008−0.025
no. droplets studied	201	80	151
droplet occupancy (%)	96.5	82	72
multiple occupancy (%)	8.5	5	9
estimated area of crystal/SAM interface, A (μm^2)	0.7−1.7	0.19−0.43	0.09−0.41
crystal volume, V (μm^3)	0.24−0.92	0.034−0.12	0.011−0.11

[a] Calculated for contact angles of 45−90° on the substrate.

therefore polymorphically identical to those precipitated in bulk solution under the same conditions. These crystals were quite different in morphology, however, in that while rhombohedral calcite crystals precipitated from the bulk solution on the SAMs, 98% of the crystals formed in the droplets (regardless of their size) were tetrahedral after 24 h of precipitation time. The crystals precipitated within the droplets were also universally smaller than those formed from the bulk solution. For example, crystals precipitated in 10 μm radius droplets displayed basal areas of ~1.2 μm^2 and edge dimensions of <2 μm, whereas crystals precipitated from the bulk solution had basal areas of >20 μm^2 and edge dimensions of 5 ± 2 μm. The orientation of the calcite crystals was also independent of the droplet diameter, and calcite crystals were predominantly observed with the {012} plane parallel to the substrate in all droplets and in the bulk solution (Figure 2c). Assessment of {012} was made by measurement of the projected interfacial angles about the threefold symmetry axis as 152, 104, and 104°, as shown in Figure 2d.[24] This orientation is consistent with the data obtained by Travaille et al.[8] for crystallization of calcite on carboxylic acid-terminated SAMs from a 9 mM $Ca(HCO_3)_2$ solution.

dx.doi.org/10.1021/ja200309m | *J. Am. Chem. Soc.* 2011, 133, 5210–5213

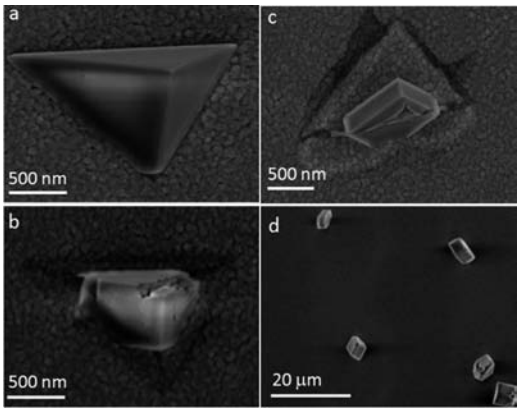

Figure 3. SEM images of (a) a calcite tetrahedron precipitated within a single 10 μm radius droplet and oriented with a {102} nucleation face; (b) the *same* particle after immersion in an undersaturated bulk solution for 90 min, with additional {104} faces visible at the vertices; (c) the transformation of a tetrahedral crystal into a rhombohedral morphology, with a trace of the original tetrahedron still visible; and (d) calcite rhombohedra formed by overgrowth of droplet-precipitated tetrahedra in a bulk solution with low supersaturation.

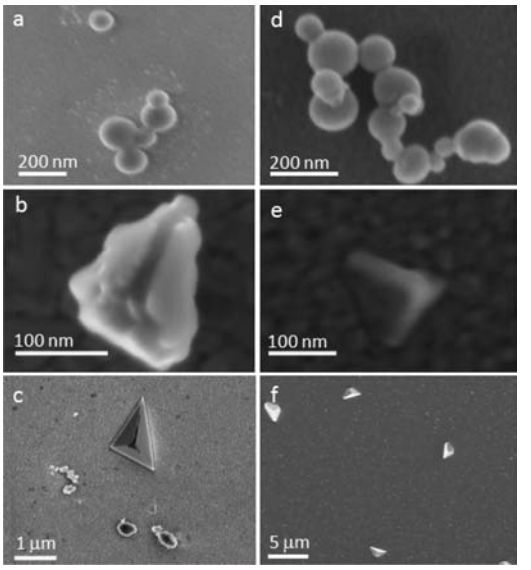

Figure 4. Short-growth-time study of (a−c) crystallization within 10 μm radius droplets and (d−f) bulk growth on homogeneous MHA SAMs. (a) Spherical, irregular particles consistent with ACC observed after 5 min. (b) Transitional particle with an irregular tetrahedral morphology observed after 30 min. (c) Single calcite tetrahedron and irregular $CaCO_3$ precipitates after 30 min. (d) Irregular, spherical particles consistent with ACC observed after 2 min. (e) A 100 nm calcite tetrahedron produced after 2 min. (f) Calcite tetrahedra observed after 15 min.

The relationship between these rhombohedral and tetrahedral morphologies was investigated by (i) slowly dissolving and (ii) further growing the tetrahedral crystals. Dissolution of the tetrahedra initiated at the vertices, generating "new" {104} faces (Figure 3a,b), and continued to give a true rhombohedron (Figure 3c). Further growth of the droplet-precipitated calcite tetrahedra in a bulk solution resulted in an order of magnitude increase in the projected edge dimensions and transformation to a rhombohedral morphology for all of the calcite particles (Figure 3d). These results very clearly show that precipitation under finite-reservoir conditions, as occurs within the droplets, effectively arrests crystal growth at an earlier stage than in bulk solution, i.e., before the tetrahedral growth form has converted into the more common rhombohedral morphology.

The droplet system was therefore explored as a means of investigating the early stages of $CaCO_3$ formation. Particles precipitated within 10 μm radius droplets were studied after short growth times and compared with precipitates formed on carboxylic acid-terminated SAMs immersed in a bulk solution at similar times (Figure 4). Spherical particles (50−200 nm diameter) that were morphologically consistent with ACC were observed at very early times in both systems (Figure 4a,d). ACC is a common precursor phase to the crystalline polymorphs of $CaCO_3$ when its saturation concentration is exceeded, and thus, its observation was not unexpected. The lifetime of the ACC precursor phase was quite different in the droplets, however. Although calcite tetrahedra, including particles with irregular, tetrahedral-based morphologies, started to appear between 5 and 30 min in the droplets (Figure 4b,c), they were evident in as little as 2 min on the surfaces immersed in the bulk solution (Figure 4e). The number of irregular particles also decreased with time, with well-defined tetrahedra being observed in ~32, 85, and 94% of the droplets after growth periods of 5, 15, and 30 min, respectively. A similar transition from ACC to tetrahedral and then to rhombohedral epitaxial calcite crystals was also observed during the precipitation of $CaCO_3$ on weathered mica substrates.[25]

The droplets therefore offer an environment where the crystals precipitate with a limited reservoir, with the vast majority supporting the growth of only one calcite crystal whose size is dictated by the total amount of $CaCO_3$ in the droplet. While we were unable to determine accurately the contact angle of such small droplets, light microscopy observations suggested that the contact angle lies in the range 45−90°. Assuming a spherical-cap configuration yielded droplet volumes in the picoliter (pL, 10^{-15} m^3) range or less (Table 1). On the basis of the tetrahedral crystal morphology, the basal area A of the calcite crystal in each droplet was estimated, and from it the volume V of a regular tetrahedron was calculated as $V \approx 0.41A^{3/2}$ (see Table 1). As can be seen, the estimated crystal volumes (in femtoliters, fL) were close to the total amount of $CaCO_3$ available in the droplets, suggesting that depletion stops further crystal growth. The environment in the droplets is therefore such that a single crystal is produced in each and that the overall population of crystals has a very narrow size distribution.

Another feature of the experiments was the formation of tetrahedral calcite crystals in the droplets. Since the equilibrium morphology of calcite is rhombohedral, it is clear that the tetrahedral crystals must represent an intermediate morphology that is favored over the rhombohedral form at small crystal sizes and stabilized by interactions with the underlying SAM.[9,26,27] No rhombohedra with dimensions of <200 nm were ever observed. $CaCO_3$ precipitation occurs by initial formation of precursor ACC particles, which adsorb and then aggregate on the substrate. Crystallization then occurs preferentially at the SAM, yielding first irregular particles and then well-defined calcite tetrahedra at particle sizes of ~100 nm. Participation of an organic matrix in ACC crystallization has been demonstrated in a number of systems, including at Langmuir monolayers,[6,10,21] and SAMs.[28,29] Further growth when a large reservoir of ions is available results in growth into the solution rather than at the substrate, supporting transformation into a rhombohedron. Within the droplets,

growth is limited by the quantity of available reactants and terminates while the particles are still tetrahedral in form.

As a final observation, we noted that while ACC is produced as a precursor phase in both the bulk solution and the droplets, formation of calcite occurs much more slowly in the droplets. This is fascinating, and a possible explanation can be provided by considering the rate of calcite nucleation on the SAMs expected in the two systems. It is emphasized that as the calcite crystals on the substrate are oriented, the transformation of ACC to calcite must occur on the SAM rather than in the bulk solution. The difference between the droplets and the bulk solution lies in the much larger ratio of substrate area to solution volume in the former system; both the composition of the solutions, including the number density of precipitated ACC, and the substrate are identical. As a result, the number density of ACC particles should be much higher for the substrate immersed in the bulk solution than for the droplets. Since the conversion rate of the ACC particles to calcite on the SAM should be proportional to the number density on the substrate, it follows that many more crystals of calcite per unit area form on the SAM in bulk solution than in the droplets. Because of its much greater thermodynamic stability, the growth of a calcite crystal after nucleation then leads to dissolution of adjacent ACC particles. This effect should be less pronounced in the droplets than in the bulk solution because of the larger average distance between a calcite crystal and the surrounding ACC particles, which ultimately leads to the longer observed lifetimes of ACC in the droplets than on the substrate immersed in the bulk solution.

In conclusion, we have here developed a method for creating picoliter droplet arrays on patterned self-assembled monolayers and employed this system to study the effects of confinement on the heterogeneous nucleation and growth of $CaCO_3$ from solution. Crystallization of the amorphous precursor ACC proceeds more slowly in the droplets than in the bulk solution. Furthermore, the restricted volumes of these droplets have a significant effect on the crystallization process, resulting in the arrest of growth at early stages; intermediate growth forms of calcite are effectively frozen in time under the limited reagent conditions. The droplet arrays therefore offer a method for studying nucleation and growth processes, which typically proceed rapidly in bulk solution, making them hard to observe without the use of sophisticated techniques such as cryogenic transmission electron microscopy[6] or X-ray scattering techniques.[21,30] This system should be of general applicability both for the investigation of different crystallizing substances and as a means of obtaining statistical data on heterogeneous nucleation. Furthermore, the results are also significant for biomineralization processes, where mineral formation occurs both within compartments and in association with organic matrices, showing that the environment in which a crystal forms can have a significant effect not only on its morphology and orientation but also on the rate of crystallization. Further work is focusing on combining this new technology with further spectroscopic and structural characterization techniques.

■ ASSOCIATED CONTENT

Supporting Information. Experimental details. This material is available free of charge via the Internet at http://pubs.acs.org.

■ AUTHOR INFORMATION

Corresponding Author
f.meldrum@leeds.ac.uk; h.k.christenson@leeds.ac.uk

■ ACKNOWLEDGMENT

We thank the EPSRC for financial support via Grant EP/E037364/2 (Y.-Y.K. and F.C.M.) and a DTA Award for C.J.S. Youmna Mouhamad is acknowledged for assistance with experiments.

■ REFERENCES

(1) Meldrum, F. C.; Colfen, H. *Chem. Rev.* **2008**, *108*, 4332.
(2) Lowenstam, H. A.; Weiner, S. *On Biomineralization*; Oxford University Press: Oxford, U.K., 1989.
(3) Elhadj, S.; De Yoreo, J. J.; Hoyer, J. R.; Dove, P. M. *Proc. Natl. Acad. Sci. U.S.A.* **2006**, *103*, 19237.
(4) Albeck, S.; Weiner, S.; Addadi, L. *Chem.—Eur. J.* **1996**, *2*, 278.
(5) Kulak, A. N.; Iddon, P.; Li, Y. T.; Armes, S. P.; Colfen, H.; Paris, O.; Wilson, R. M.; Meldrum, F. C. *J. Am. Chem. Soc.* **2007**, *129*, 3729.
(6) Pouget, E. M.; Bomans, P. H. H.; Goos, J. A. C. M.; Frederik, P. M.; de With, G.; Sommerdijk, N. A. J. M. *Science* **2009**, *323*, 1455.
(7) Aizenberg, J.; Black, A. J.; Whitesides, G. M. *Nature* **1999**, *398*, 495.
(8) Travaille, A. M.; Kaptijn, L.; Verwer, P.; Hulsken, B.; Elemans, J.; Nolte, R. J. M.; van Kempen, H. *J. Am. Chem. Soc.* **2003**, *125*, 11571.
(9) Loste, E.; Diaz-Marti, E.; Zarbakhsh, A.; Meldrum, F. C. *Langmuir* **2003**, *19*, 2830.
(10) Pichon, B. P.; Bomans, P. H. H.; Frederik, P. M.; Sommerdijk, N. *J. Am. Chem. Soc.* **2008**, *130*, 4034.
(11) Stephens, C. J.; Ladden, S. F.; Meldrum, F. C.; Christenson, H. K. *Adv. Funct. Mater.* **2010**, *20*, 2108.
(12) Loste, E.; Park, R. J.; Warren, J.; Meldrum, F. C. *Adv. Funct. Mater.* **2004**, *14*, 1211.
(13) Finnemore, A. S.; Scherer, M. R. J.; Langford, R.; Mahajan, S.; Ludwigs, S.; Meldrum, F. C.; Steiner, U. *Adv. Mater.* **2009**, *21*, 3928.
(14) Wucher, B.; Yue, W. B.; Kulak, A. N.; Meldrum, F. C. *Chem. Mater.* **2007**, *19*, 1111.
(15) Goh, L.; Chen, K. J.; Bhamidi, V.; He, G. W.; Kee, N. C. S.; Kenis, P. J. A.; Zukoski, C. F.; Braatz, R. D. *Cryst. Growth Des.* **2010**, *10*, 2515.
(16) Murray, B. J.; Broadley, S. L.; Wilson, T. W.; Bull, S.; Wills, R. H.; Christenson, H. K.; Murray, E. J. *Phys. Chem. Chem. Phys.* **2010**, *12*, 10180.
(17) Chayen, N. E.; Shaw Stewart, P. D.; Blow, D. M. *J. Cryst. Growth* **1992**, *122*, 176.
(18) Galkin, O.; Vekilov, P. G. *J. Am. Chem. Soc.* **2000**, *122*, 156.
(19) Song, H.; Chen, D. L.; Ismagilov, R. F. *Angew. Chem., Int. Ed.* **2006**, *45*, 7336.
(20) Leng, J.; Salmon, J. B. *Lab Chip* **2009**, *9*, 24.
(21) Wolf, S. E.; Leiterer, J.; Kappl, M.; Emmerling, F.; Tremel, W. *J. Am. Chem. Soc.* **2008**, *130*, 12342.
(22) Lee, A. Y.; Lee, I. S.; Myerson, A. S. *Chem. Eng. Technol.* **2006**, *29*, 281.
(23) Lee, I. S.; Kim, K. T.; Lee, A. Y.; Myerson, A. S. *Cryst. Growth Des.* **2008**, *8*, 108.
(24) Archibald, D. D.; Qadri, S. B.; Gaber, B. P. *Langmuir* **1996**, *12*, 538.
(25) Stephens, C. J.; Mouhamad, Y.; Meldrum, F. C.; Christenson, H. K. *Cryst. Growth Des.* **2010**, *10*, 734.
(26) Heywood, B. R.; Mann, S. *Adv. Mater.* **1994**, *6*, 9.
(27) Pokroy, B.; Aizenberg, J. *CrystEngComm* **2007**, *9*, 1219.
(28) Han, T. Y. J.; Aizenberg, J. *Chem. Mater.* **2008**, *20*, 1064.
(29) Lee, J. R. I.; Han, T. Y. J.; Willey, T. M.; Wang, D.; Meulenberg, R. W.; Nilsson, J.; Dove, P. M.; Terminello, L. J.; van Buuren, T.; De Yoreo, J. J. *J. Am. Chem. Soc.* **2007**, *129*, 10370.
(30) Bolze, J.; Pontoni, D.; Ballauff, M.; Narayanan, T.; Colfen, H. *J. Colloid Interface Sci.* **2004**, *277*, 84.